



Ca/Sr ratio dependent structure and up-conversion luminescence of $(\text{Ca}_{1-x}\text{Sr}_x)\text{In}_2\text{O}_4$: $\text{Yb}^{3+}/\text{Ho}^{3+}$ phosphors

Journal:	<i>RSC Advances</i>
Manuscript ID:	RA-ART-05-2015-008467.R1
Article Type:	Paper
Date Submitted by the Author:	01-Jul-2015
Complete List of Authors:	Guan, Ming; China University of Geosciences (Beijing) Beijing, Zheng, Hong; China University of Geosciences, Beijing, School of Materials Science and Technology Huang, Zhaohui; China University of Geosciences (Beijing), School of Materials Science and Technology Ma, Bin; China University of Geosciences (Beijing), School of Materials Science and Technology Beijing, China Molokeev, Maxim; Kirensky Institute of Physics, SB RAS, Huang, Saifang; The University of Auckland, Department of Chemical & Materials Engineering; China University of Geosciences (Beijing), School of Materials Science and Technology Mei, Lefu; China University of Geosciences, Materials Science and Technology



Journal Name

ARTICLE

Ca/Sr ratio dependent structure and up-conversion luminescence of $(\text{Ca}_{1-x}\text{Sr}_x)\text{In}_2\text{O}_4$: $\text{Yb}^{3+}/\text{Ho}^{3+}$ phosphors

Received 00th January 20xx,
Accepted 00th January 20xx

DOI: 10.1039/x0xx00000x

www.rsc.org/

Ming Guan,^a Hong Zheng,^{a†} Zhaohui Huang,^a Bin Ma,^a Maxim S. Molokeev,^b Saifang Huang^c and Lefu Mei^{a†}

Up-conversion (UC) phosphors of $(\text{Ca}_{1-x}\text{Sr}_x)\text{In}_2\text{O}_4$: $\text{Yb}^{3+}/\text{Ho}^{3+}$ ($x = 0, 0.1, 0.3, 0.5, 0.7, 0.9, 1.0$) were prepared. Based on the crystal structure evolution of these series solid solution samples, which were characterized by Rietveld refinement, the variation of UC luminescent properties was discussed in detail. Sr and Ca occupied one position and Yb/Ho dissolved in the In site in the $(\text{Ca}_{1-x}\text{Sr}_x)\text{In}_2\text{O}_4$ lattice. With increasing Sr substituting Ca atoms, the cell parameters and cell volumes of these samples increased linearly, and distortions of $(\text{Ca}/\text{Sr})\text{O}_8$ polyhedron were formed. The distortions on crystal structures showed a negative relation with UC luminescent intensities in these series phosphors.

Introduction

The study of up-conversion (UC) phosphors has attracted great attention recently due to its significant potential application in light emitting displays, solid-state lasers, biological labelling, solar energy conversion, and so on.^{1, 2} As spectral modification materials, UC phosphors showed great importance for converting multiple photons of lower energy into one photon of high energy according to Anti-Stokes emission processes. Intense UC luminescence from infrared to visible light was observed widely in many UC phosphors.³⁻⁵

Recently, some studies showed that the luminescence of ultra-violet excited phosphors always was affected greatly by its crystal structure.⁶⁻¹⁰ However, the mechanism of how the crystal structure influences the optical properties of UC materials is still not clear enough. In order to study the relationships between UC luminescence properties and crystal structures, $\text{Yb}^{3+}/\text{Ho}^{3+}$ co-doped $(\text{Ca}_{1-x}\text{Sr}_x)\text{In}_2\text{O}_4$, as well as CaIn_2O_4 and SrIn_2O_4 were prepared. Indium (In) belongs to the same group with boron, aluminum and gallium, it was suggested as an excellent host lattice for luminescence.^{11, 12} Recent reports showed that $\text{Yb}^{3+}/\text{Ho}^{3+}$ co-doped CaIn_2O_4 and SrIn_2O_4 have excellent UC luminescent properties. CaIn_2O_4 and SrIn_2O_4 have low phonon energies ($\sim 475 \text{ cm}^{-1}$), which is much lower than those of other typical oxide hosts, such as Y_2O_3 ($\sim 600 \text{ cm}^{-1}$), silicate ($\sim 1100 \text{ cm}^{-1}$), they can therefore achieve high-efficiency UC emissions.¹³⁻¹⁷ Previously, the structure of CaIn_2O_4 was discussed in literatures, but no correct ICSD (Inorganic Crystal Structure Database) or JCPDS (Joint Committee on Powder Diffraction Standards) file for the CaIn_2O_4 is available.¹² In the SrIn_2O_4 structure (orthorhombic, *Pnma*, ICSD #16241), two kinds of distorted InO_6

octahedra were connected to form a network, and Sr^{2+} ions located in the middle of the formed pentagonal prism tunnel. As the similarity of Ca^{2+} and Sr^{2+} ions, $(\text{Ca}_{1-x}\text{Sr}_x)\text{In}_2\text{O}_4$ shows great potential in the formation of continuous solid solution. As the difference, replacement between Ca and Sr are expected to change the crystal structure slightly and then influence the UC luminescent properties of UC phosphors. For Ho^{3+} and Yb^{3+} ions, they are important activator and sensitizer for UC phosphors, respectively.¹⁸⁻²⁰

In this work, UC phosphors of $\text{Yb}^{3+}/\text{Ho}^{3+}$ co-doped $(\text{Ca}_{1-x}\text{Sr}_x)\text{In}_2\text{O}_4$ continuous solid solution phosphors were synthesized via a solid-state reaction process. According to our previous result, the ratio of $\text{Yb}^{3+}/\text{Ho}^{3+}$ was determined as 0.1/0.005 to get a good UC luminescence.¹⁴ The relationship between crystal structure evolution and UC luminescent properties of this series samples were discussed in detail.

Experimental

Starting materials of CaCO_3 (A.R.), SrCO_3 (A.R.), In_2O_3 (99.995%), Yb_2O_3 (99.995%), Ho_2O_3 (99.995%), Yb_2O_3 (99.995%) were weighted according to stoichiometric ratio, and then the mixtures were ground thoroughly in an agate mortar. After that, the mixtures were sintered at 1300°C for 3 hours, with the heating rate of $5^\circ\text{C}/\text{min}$, and then cooled to room temperature naturally. All the samples were washed for three times by the deionized water and dried for the following measurement.

The X-ray powder diffractometer (D8-ADVANCE, Bruker Corporation, Germany) with Cu-K α and linear VANTEC detector was used for Rietveld analysis. The step size of 2θ was 0.02° , and the counting time was 2s per step. Rietveld refinement was performed by using TOPAS 4.2.²¹ The UC luminescent spectra were recorded on a spectrophotometer (F-4600, Hitachi, Japan) equipped with an external power-controllable 980nm semiconductor laser (Beijing Viasho Technology Company, China) as the excitation source. Diffuse reflection spectra were measured on a UV-vis-NIR spectrophotometer (Shimadzu UV-3600, Japan) attached to an integral sphere, and BaSO_4 was used as a reference standard. All the measurements were carried out at room temperature.

^a School of Materials Science and Technology, Beijing Key Laboratory of Materials Utilization of Nonmetallic Minerals and Solid Wastes, National Laboratory of Mineral Materials, China University of Geosciences, Beijing 100083, China.

^b Laboratory of Crystal Physics, Kirensky Institute of Physics, SB RAS, Krasnoyarsk 660036, Russia.

^c Department of Chemical and Materials Engineering, the University of Auckland, PB 92019, Auckland 1142, New Zealand.

† E-mail: zhengh@cugb.edu.cn and mlf@cugb.edu.cn

Results and discussion

X-ray diffraction (XRD) was employed to characterize the structure evolution of all the $0.1\text{Yb}^{3+}/0.005\text{Ho}^{3+}$ doped $(\text{Ca}_{1-x}\text{Sr}_x)\text{In}_2\text{O}_4$ ($x = 0, 0.1, 0.3, 0.5, 0.7, 0.9, 1.0$) samples. Figure 1 showed the selected XRD patterns of $(\text{Ca}_{0.5}\text{Sr}_{0.5})\text{In}_2\text{O}_4: \text{Yb}^{3+}/\text{Ho}^{3+}$ sample, as well as pure CaIn_2O_4 and SrIn_2O_4 . Because of no correct ICSD or JCPDS file for the CaIn_2O_4 is available, all X-ray pattern of $(\text{Ca}_{1-x}\text{Sr}_x)\text{In}_2\text{O}_4: \text{Yb}^{3+}/\text{Ho}^{3+}$ were indexed by orthorhombic cell ($Pnma$) with parameters close to SrIn_2O_4 (ICSD #16241), so this crystal structure was used to make Rietveld refinement. In crystal structure there is only one position which can be occupied by Sr and Ca, and this position is multiplied by four positions by symmetry elements (Figure 2). The occupations of Sr/Ca ions were fixed during refinement. Also Yb^{3+} and Ho^{3+} ions are dissolved in the lattice and substituted In^{3+} ions partly, and their occupancies were fixed. The refinement of all the samples $(\text{Ca}_{1-x}\text{Sr}_x)\text{In}_2\text{O}_4: \text{Yb}^{3+}/\text{Ho}^{3+}$, pure CaIn_2O_4 and SrIn_2O_4 were stable, and ended with low R-factors (shown in Table 1, Figure 1). $(\text{Ca}/\text{Sr})\text{O}_8$ square antiprism and $(\text{In}/\text{Yb}/\text{Ho})\text{O}_6$ octahedra are existed in the crystal structure simultaneously. The detailed crystal structure of $(\text{Ca}_{1-x}\text{Sr}_x)\text{In}_2\text{O}_4: 0.1\text{Yb}^{3+}/0.005\text{Ho}^{3+}$ is shown in Figure 2.

Figure 3 showed the refined lattice parameters of a , b , c , and

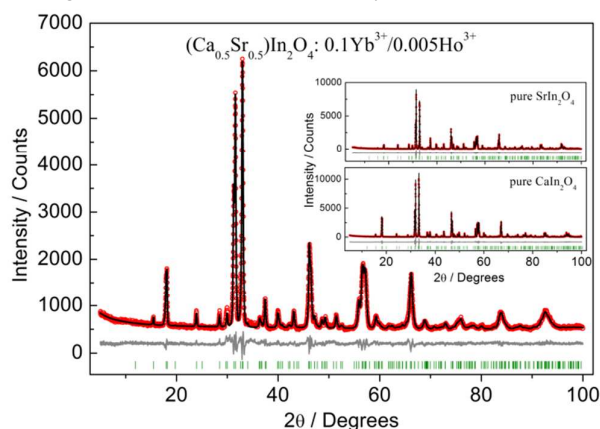


Figure 1. Observed (red), calculated (black), and difference (gray) XRD pattern for the refinement of $(\text{Ca}_{0.5}\text{Sr}_{0.5})\text{In}_2\text{O}_4: 0.1\text{Yb}^{3+}/0.005\text{Ho}^{3+}$, as well as pure CaIn_2O_4 and SrIn_2O_4 samples in the insets

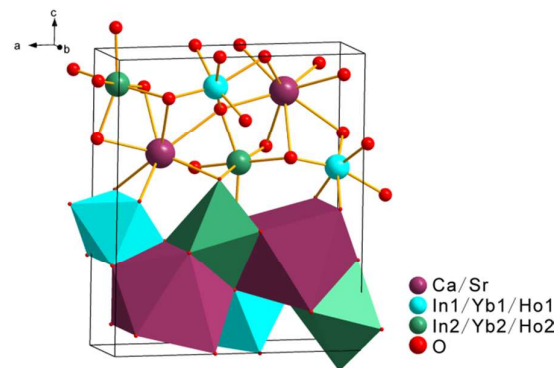


Figure 2. Crystal structure of the $(\text{Ca}_{1-x}\text{Sr}_x)\text{In}_2\text{O}_4: 0.1\text{Yb}^{3+}/0.005\text{Ho}^{3+}$ samples

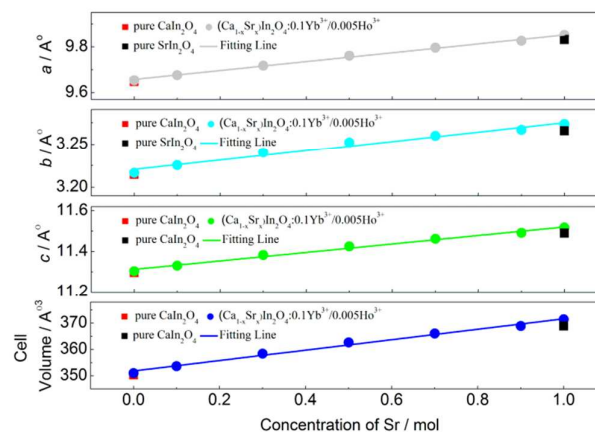


Figure 3. Refined lattice parameter of a , b , c , and unit cell volume (V) showed a linear increase as function of x values in $(\text{Ca}_{1-x}\text{Sr}_x)\text{In}_2\text{O}_4: \text{Yb}^{3+}/\text{Ho}^{3+}$ ($x = 0, 0.1, 0.3, 0.5, 0.7, 0.9, 1.0$), and a , b , c , V values in pure CaIn_2O_4 and SrIn_2O_4

unit cell volume (V) as functions of x values in $(\text{Ca}_{1-x}\text{Sr}_x)\text{In}_2\text{O}_4: \text{Yb}^{3+}/\text{Ho}^{3+}$ ($x = 0, 0.1, 0.3, 0.5, 0.7, 0.9, 1.0$) samples, and a , b , c , and V value in pure CaIn_2O_4 and SrIn_2O_4 . Since Ca/Sr in eight coordination, and the ionic radii $\text{IR}(\text{Ca}^{2+}, \text{CN}=8) = 1.12\text{Å}$, $\text{IR}(\text{Sr}^{2+}, \text{CN}=8) = 1.26\text{Å}$,²² lattice parameters of a , b , c and V of these samples

Table 1. Main parameters of processing and refinement of $(\text{Ca}_{1-x}\text{Sr}_x)\text{In}_2\text{O}_4: 0.1\text{Yb}^{3+}/0.005\text{Ho}^{3+}$, pure CaIn_2O_4 and SrIn_2O_4 samples

Compounds	Space Group	a , Å	b , Å	c , Å	V , Å ³	R_{wp} , %
CaIn_2O_4	$Pnma$	9.64847 (10)	3.21443(3)	11.29593 (11)	350.336 (6)	11.14
$\text{CaIn}_2\text{O}_4: 0.1\text{Yb}^{3+}, 0.005\text{Ho}^{3+}$	$Pnma$	9.6543 (2)	3.21652(8)	11.3034 (3)	351.007 (15)	12.29
$(\text{Ca}_{0.9}\text{Sr}_{0.1})\text{In}_2\text{O}_4: 0.1\text{Yb}^{3+}, 0.005\text{Ho}^{3+}$	$Pnma$	9.6768 (4)	3.22542(13)	11.3307 (4)	353.65 (2)	11.65
$(\text{Ca}_{0.7}\text{Sr}_{0.3})\text{In}_2\text{O}_4: 0.1\text{Yb}^{3+}, 0.005\text{Ho}^{3+}$	$Pnma$	9.7180 (5)	3.24012(16)	11.3826 (6)	358.41 (3)	9.96
$(\text{Ca}_{0.5}\text{Sr}_{0.5})\text{In}_2\text{O}_4: 0.1\text{Yb}^{3+}, 0.005\text{Ho}^{3+}$	$Pnma$	9.7613 (5)	3.25218(17)	11.4253 (6)	362.70 (3)	10.17
$(\text{Ca}_{0.3}\text{Sr}_{0.7})\text{In}_2\text{O}_4: 0.1\text{Yb}^{3+}, 0.005\text{Ho}^{3+}$	$Pnma$	9.7967 (4)	3.25980(12)	11.4624 (4)	366.06 (2)	9.33
$(\text{Ca}_{0.1}\text{Sr}_{0.9})\text{In}_2\text{O}_4: 0.1\text{Yb}^{3+}, 0.005\text{Ho}^{3+}$	$Pnma$	9.8266 (3)	3.26668(10)	11.4917 (3)	368.886 (19)	11.05
$\text{SrIn}_2\text{O}_4: 0.1\text{Yb}^{3+}, 0.005\text{Ho}^{3+}$	$Pnma$	9.85194 (17)	3.27340(6)	11.5178 (2)	371.443 (11)	9.08
SrIn_2O_4	$Pnma$	9.83188 (9)	3.26563(3)	11.49003 (11)	368.914 (6)	10.14

showed a linear increase with the increasing Sr content, indicating that the $(\text{Ca}_{1-x}\text{Sr}_x)\text{In}_2\text{O}_4$ formed continuous solid solution. Moreover, pure CaIn_2O_4 and SrIn_2O_4 have smaller lattice parameters and cell volumes than $\text{Yb}^{3+}/\text{Ho}^{3+}$ co-doped CaIn_2O_4 and SrIn_2O_4 , respectively. This is because $\text{In}/\text{Yb}/\text{Ho}$ in six coordination, and IR (Yb^{3+} , CN=6) = 0.868 Å, IR (Ho^{3+} , CN=6) = 0.901 Å, IR (In^{3+} , CN=6) = 0.8 Å; $\text{Yb}^{3+}/\text{Ho}^{3+}$ dopants in CaIn_2O_4 or SrIn_2O_4 enlarged the unit cells due to their larger IR than In^{3+} , testifying that Yb^{3+} and Ho^{3+} ions occupied the In^{3+} ions sites.

Figure 4 gave the UC emission spectra of pure CaIn_2O_4 , $(\text{Ca}_{1-x}\text{Sr}_x)\text{In}_2\text{O}_4: 0.1\text{Yb}^{3+}/0.005\text{Ho}^{3+}$ ($x = 0, 0.1, 0.3, 0.5, 0.7, 0.9, 1.0$), and SrIn_2O_4 upon 980 nm laser excitation. Lacking of rare earth sensitive and active ions, no UC emission was observed in pure CaIn_2O_4 and SrIn_2O_4 samples. For $(\text{Ca}_{1-x}\text{Sr}_x)\text{In}_2\text{O}_4: \text{Yb}^{3+}/\text{Ho}^{3+}$, strong green emission with the strongest peak at 546 nm was obtained, which was associated with the characteristic energy level transition of $^5\text{S}_2(^5\text{F}_4) \rightarrow ^5\text{I}_8$ of Ho^{3+} .^{13, 17, 23} $\text{SrIn}_2\text{O}_4: \text{Yb}^{3+}/\text{Ho}^{3+}$ showed the strongest UC luminescence among all the samples, suggesting that SrIn_2O_4 would be an excellent UC host material. Nevertheless, it can be seen that majority of Ca/Sr ratio substituted samples

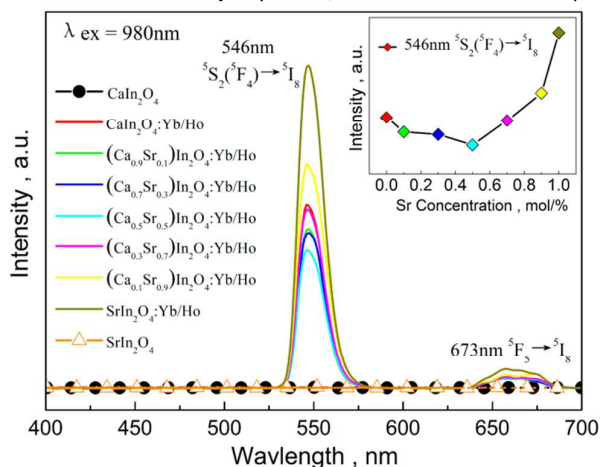


Figure 4. UC emission spectra of pure CaIn_2O_4 , $(\text{Ca}_{1-x}\text{Sr}_x)\text{In}_2\text{O}_4: 0.1\text{Yb}^{3+}/0.005\text{Ho}^{3+}$ ($x = 0, 0.1, 0.3, 0.5, 0.7, 0.9, 1.0$), and SrIn_2O_4 upon 980 nm laser excitation, and the inset shows the variation of UC emission intensities

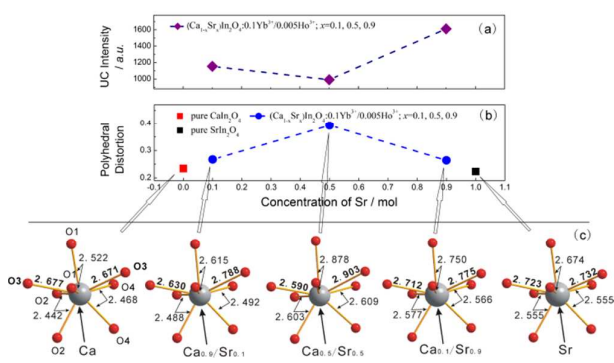


Figure 5. UC emission intensities at 546 nm of $(\text{Ca}_{1-x}\text{Sr}_x)\text{In}_2\text{O}_4: 0.1\text{Yb}^{3+}/0.005\text{Ho}^{3+}$ ($x = 0.1, 0.5, 0.9$) (a); Calculated distortion indexes of $(\text{Ca}/\text{Sr})\text{O}_8$ polyhedron in pure CaIn_2O_4 , $(\text{Ca}_{1-x}\text{Sr}_x)\text{In}_2\text{O}_4: 0.1\text{Yb}^{3+}/0.005\text{Ho}^{3+}$ ($x = 0.1, 0.5, 0.9$), and pure SrIn_2O_4 (b); $(\text{Ca}/\text{Sr})\text{O}_8$ polyhedron of pure CaIn_2O_4 , $\text{Ca}_{1-x}\text{Sr}_x\text{In}_2\text{O}_4: 0.1\text{Yb}^{3+}/0.005\text{Ho}^{3+}$ ($x = 0.1, 0.5, 0.9$), and pure SrIn_2O_4 (c)

possessed lower UC luminescent intensities than $\text{CaIn}_2\text{O}_4: \text{Yb}^{3+}/\text{Ho}^{3+}$ and $\text{SrIn}_2\text{O}_4: \text{Yb}^{3+}/\text{Ho}^{3+}$ samples.

In order to explain the UC emission intensity differences in Ca/Sr ratio substituted samples, the detailed crystal structures and polyhedrons of some samples were analysed. The $(\text{Ca}/\text{Sr})\text{O}_8$ polyhedral distortion index, D , can be calculated as followed:

$$D = \frac{1}{n} \sum_{i=1}^n \frac{|l_i - l_{av}|}{l_{av}} \quad (1)$$

where l_i is the distance between central atom and the i th coordinating atom, and the l_{av} is the mean bond length.⁷ The calculated distortion of pure CaIn_2O_4 , $(\text{Ca}_{1-x}\text{Sr}_x)\text{In}_2\text{O}_4: \text{Yb}^{3+}/\text{Ho}^{3+}$ ($x = 0.1, 0.5, 0.9$), and pure SrIn_2O_4 were determined as 0.234, 0.267, 0.392, 0.264, 0.223, respectively. With the increased Sr substituting Ca, the UC emission intensities of $(\text{Ca}_{1-x}\text{Sr}_x)\text{In}_2\text{O}_4: \text{Yb}^{3+}/\text{Ho}^{3+}$ decreased firstly and then increased, as shown in Figure 5. (a). Meanwhile, the crystal structures of $(\text{Ca}_{1-x}\text{Sr}_x)\text{In}_2\text{O}_4: \text{Yb}^{3+}/\text{Ho}^{3+}$ became distort with the substitution between Ca/Sr, and the distortions enlarged firstly and then reduced, as shown in Figure 5. (b). In Figure 5. (c), the distortions also can be observed from the variations of Ca-O3 bond distances: 2.677 and 2.671 in pure CaIn_2O_4 , 2.590 and 2.903 in $(\text{Ca}_{0.5}\text{Sr}_{0.5})\text{In}_2\text{O}_4: \text{Yb}^{3+}/\text{Ho}^{3+}$, 2.723 and 2.732 in pure SrIn_2O_4 .

Fig. 6 gives the diffuse reflection spectra of pure CaIn_2O_4 , $\text{Ca}_{1-x}\text{Sr}_x\text{In}_2\text{O}_4: 0.1\text{Yb}^{3+}/0.005\text{Ho}^{3+}$ ($x = 0.1, 0.5, 0.9$), and pure SrIn_2O_4 samples. No absorption bands except for UV region were found in the non-doped CaIn_2O_4 and SrIn_2O_4 . However, absorption valley centred at 449, 540, 643 nm (Ho^{3+} ions) and 980 nm (Yb^{3+} ions) were observed. In $\text{Yb}^{3+}/\text{Ho}^{3+}$ doped UC phosphors, two channels of excitations are responsible for the impurity luminescence. One is direct excitation of Ho^{3+} ions. The other is indirect excitation, followed by an energy transfer from the Yb^{3+} to the Ho^{3+} ions to cause the luminescence. The three diffuse reflection patterns of $\text{Yb}^{3+}/\text{Ho}^{3+}$ co-doped $\text{Ca}_{1-x}\text{Sr}_x\text{In}_2\text{O}_4$ ($x = 0.1, 0.5, 0.9$) are similar, revealing that the substitution between Ca and Sr did not change the UC luminescence mechanism for Ho^{3+} or $\text{Yb}^{3+}/\text{Ho}^{3+}$.

Accordingly, a new model that the distortion (D) of $(\text{Ca}/\text{Sr})\text{O}_8$ polyhedron has a negative relation with UC luminescent intensity (I) in $(\text{Ca}_{1-x}\text{Sr}_x)\text{In}_2\text{O}_4: \text{Yb}^{3+}/\text{Ho}^{3+}$ samples was proposed:

$$I \propto \frac{1}{D} \quad (2)$$

The lattice expansion and increased distortion cause by partial substitution for Ca/Sr changed the crystal field acting on the Ho^{3+}

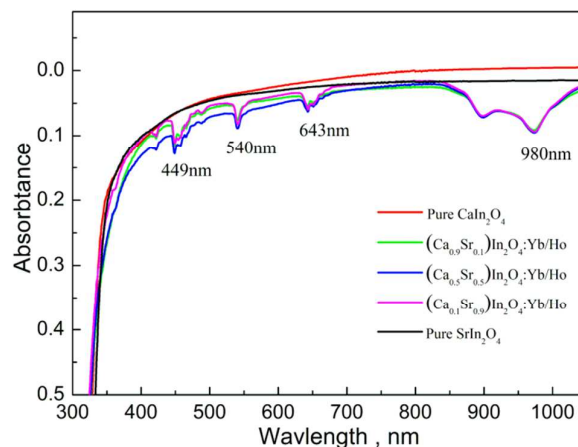


Figure 6. The diffuse reflection spectra of pure CaIn_2O_4 , $\text{Ca}_{1-x}\text{Sr}_x\text{In}_2\text{O}_4: 0.1\text{Yb}^{3+}/0.005\text{Ho}^{3+}$ ($x = 0.1, 0.5, 0.9$), and pure SrIn_2O_4

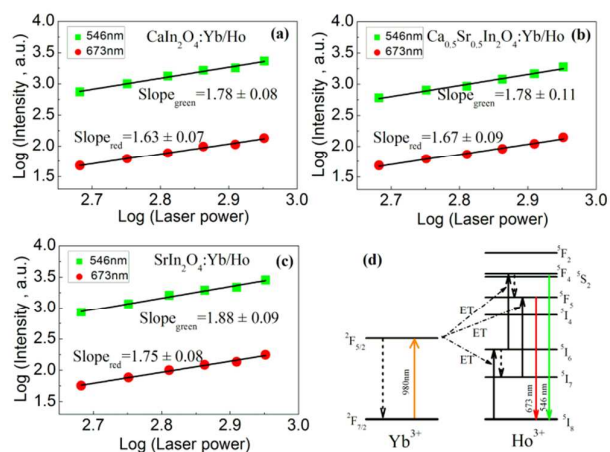


Figure 7. Dependence of UC emission intensities upon different pumping powers of $\text{CaIn}_2\text{O}_4: 0.1\text{Yb}^{3+}/0.005\text{Ho}^{3+}$ (a), $(\text{Ca}_{0.5}\text{Sr}_{0.5})\text{In}_2\text{O}_4: 0.1\text{Yb}^{3+}/0.005\text{Ho}^{3+}$ (b), $\text{SrIn}_2\text{O}_4: 0.1\text{Yb}^{3+}/0.005\text{Ho}^{3+}$ (c), and proposed UC luminescence mechanisms in $\text{Yb}^{3+}/\text{Ho}^{3+}$ doped $(\text{Ca}_{1-x}\text{Sr}_x)\text{In}_2\text{O}_4$ phosphors

or $\text{Yb}^{3+}/\text{Ho}^{3+}$ ions,^{24,25} leading to the variation of UC luminescent properties in the $\text{Yb}^{3+}/\text{Ho}^{3+}$ co-doped $(\text{Ca}_{1-x}\text{Sr}_x)\text{In}_2\text{O}_4$ continuous solid solution phosphors.

Figure 7 showed the dependence of UC emission intensities upon different pumping powers of $\text{CaIn}_2\text{O}_4: \text{Yb}^{3+}/\text{Ho}^{3+}$ (a), typical $(\text{Ca}_{0.5}\text{Sr}_{0.5})\text{In}_2\text{O}_4: \text{Yb}^{3+}/\text{Ho}^{3+}$ (b), and $\text{SrIn}_2\text{O}_4: \text{Yb}^{3+}/\text{Ho}^{3+}$ (c). In $(\text{Ca}_{0.5}\text{Sr}_{0.5})\text{In}_2\text{O}_4: \text{Yb}^{3+}/\text{Ho}^{3+}$ sample, the double logarithmic plot of the integrated intensities of emissions at 546nm ($^2\text{S}_2/{}^3\text{F}_4 \rightarrow {}^5\text{I}_8$) and 673nm (${}^2\text{F}_5 \rightarrow {}^5\text{I}_8$) versus the pump powers yields two straight lines with slopes of 1.78 ± 0.11 and 1.67 ± 0.09 , respectively. Furthermore, the slopes were determined as 1.78 ± 0.08 and 1.63 ± 0.07 in $\text{CaIn}_2\text{O}_4: \text{Yb}^{3+}/\text{Ho}^{3+}$, as well as 1.88 ± 0.09 and 1.75 ± 0.08 in $\text{SrIn}_2\text{O}_4: \text{Yb}^{3+}/\text{Ho}^{3+}$. These slopes indicated that the UC emissions in all $\text{Yb}^{3+}/\text{Ho}^{3+}$ co-doped $(\text{Ca}_{1-x}\text{Sr}_x)\text{In}_2\text{O}_4$ UC phosphors are two-photon process. Figure 7 (d) proposed the UC luminescence mechanism of these $\text{Yb}^{3+}/\text{Ho}^{3+}$ co-doped phosphors. In the present system, the excited Yb^{3+} ions transferred its energy to neighbouring Ho^{3+} ion through energy transfer (ET) process ${}^2\text{F}_{5/2}(\text{Yb}^{3+}) + {}^5\text{I}_8(\text{Ho}^{3+}) \rightarrow {}^2\text{F}_{7/2}(\text{Yb}^{3+}) + {}^5\text{I}_6(\text{Ho}^{3+})$, ${}^2\text{F}_{5/2}(\text{Yb}^{3+}) + {}^5\text{I}_6(\text{Ho}^{3+}) \rightarrow {}^2\text{F}_{7/2}(\text{Yb}^{3+}) + {}^5\text{F}_4/{}^5\text{S}_2(\text{Ho}^{3+})$, ${}^2\text{F}_{5/2}(\text{Yb}^{3+}) + {}^5\text{I}_7(\text{Ho}^{3+}) \rightarrow {}^2\text{F}_{7/2}(\text{Yb}^{3+}) + {}^7\text{F}_5(\text{Ho}^{3+})$, and then the excited Ho^{3+} ion emit green emissions (546 nm, ${}^5\text{S}_2/{}^5\text{F}_4 \rightarrow {}^5\text{I}_8$) and red emission (673nm, ${}^5\text{F}_5 \rightarrow {}^5\text{I}_8$).

Conclusions

Ca/Sr ratio dependent structure and up-conversion luminescence of $(\text{Ca}_{1-x}\text{Sr}_x)\text{In}_2\text{O}_4: \text{Yb}^{3+}/\text{Ho}^{3+}$ ($x = 0, 0.1, 0.3, 0.5, 0.7, 0.9, 1.0$) phosphors were studied in detail, and the structure evolution of these series samples were showed by Rietveld refinement. With increasing Sr atoms substituting Ca in the $(\text{Ca}_{1-x}\text{Sr}_x)\text{In}_2\text{O}_4$ lattice, the cell parameters and cell volumes of these samples increase linearly. Sr^{2+} and Ca^{2+} occupied one position and $\text{Yb}^{3+}/\text{Ho}^{3+}$ dissolved in the In^{3+} site. Since the differences between Sr^{2+} and Ca^{2+} , $(\text{Ca}/\text{Sr})\text{O}_8$ polyhedron distortions were formed, and these distortions suggested a negative relation with UC luminescent intensities in these series phosphors. The UC

luminescent properties, pumping powers study and possible UC mechanism of these samples also were discussed.

Acknowledgements

This present work was supported by the National Natural Science Foundations of China (Grant No. 51202226), the Fundamental Research Funds for the Central Universities (Grant No. 2652014125, 2652013128, 2652013043), and the Research Fund for the Doctoral Program of Higher Education of China (Grant No. 20130022110006).

Notes and references

- 1 R. Martín-Rodríguez, S. Fischer, A. Ivaturi, B. Froehlich, K.W. Krämer, J.C. Goldschmidt, B.S. Richards and A. Meijerink, *Chemistry of Materials*, 2013, **25**, 1912;
- 2 F. Wang and X. Liu, Chemical Society reviews, *Chemical Society reviews*, 2009, **38**, 976;
- 3 Z.G. Xia, P. Du and L.B. Liao. *Phys. Status Solidi A*, 2013, **210**, 1734;
- 4 A.I. Orlova, S.N. Pleskova, N.V. Malanina, A.N. Shushunov, E.N. Gorshkova, E.E. Pudovkina and O.N. Gorshkov, *Inorganic Materials*, 2013, **49**, 696;
- 5 Z. Xia, J. Li, Y. Luo, L. Liao and J. Varela, *Journal of the American Ceramic Society*, 2012, **95**, 3229;
- 6 X. Yu, Y. Qin, M. Gao, L. Duan, Z. Jiang, L. Gou, P. Zhao and Z. Li, *Journal of Luminescence*, 2014, **153**, 1;
- 7 K.A. Denault, J. Brgoch, M.W. Gaultois, A. Mikhailovsky, R. Petry, H. Winkler, S.P. DenBaars and R. Seshadri, *Chemistry of Materials*, 2014, **26**, 2275;
- 8 F. Cheng, Z. Xia, X. Jing and Z. Wang, *Phys Chem Chem Phys.*, 2015, **17**, 3689;
- 9 H. Ji, Z. Huang, Z. Xia, M.S. Molokeev, X. Jiang, Z. Lin and V.V. Atuchin, *Dalton transactions*, 2015;
- 10 H. Ji, Z. Huang, Z. Xia, M.S. Molokeev, V.V. Atuchin, M. Fang and S. Huang, *Inorganic chemistry*, 2014, **53**, 5129;
- 11 A. Baszczuk, M. Jasiorski, M. Nyk, J. Hanuza, M. Mączka and W. Stręk, *Journal of Alloys and Compounds*, 2005, **394**, 88;
- 12 J.W. Tang, Z.G. Zou and J.H. Ye, *Chem. Mater.*, 2004, **16**, 1644;
- 13 T. Li, C. Guo, Y. Yang, L. Li and N. Zhang, *Acta Materialia*, 2013, **61**, 7481;
- 14 M. Guan, H. Zheng, L. Mei, Z. Huang, T. Yang, M. Fang and Y. Liu, *Infrared Physics & Technology*, 2014, **67**, 107;
- 15 T. Li, C. Guo and L. Li, *Optics express*, 2013, **21**, 18281;
- 16 M. Guan, H. Zheng, L. Mei, M.S. Molokeev, J. Xie, T. Yang, X. Wu, S. Huang and Z. Huang, *Journal of the American Ceramic Society*, 2015, **98**, 1182;
- 17 25 F. Kang, X. Yang, M. Peng, L. Wondraczek, Z. Ma and J. Qiu, *Journal of Physical Chemistry C*, 2014, **118**, 7515;
- 18 X. Li, J. Zhu, Z. Man, Y. Ao and H. Chen, *Scientific reports*, 2014, **4**, 4446;
- 19 R. Martín-Rodríguez and A. Meijerink, *Journal of Luminescence*, 2014, **147**, 147;
- 20 M. Peng and L. Wondraczek, *Journal of the American Ceramic Society*, 2010, **93**, 1437;
- 21 Bruker AXS TOPAS V4 – User’s Manual. Bruker AXS, Karlsruhe, Germany. 2008;
- 22 R.D. Shannon, *Acta Cryst. A*, 1976, **32**, 751;
- 23 S. Zhou, S. Jiang, X. Wei, Y. Chen, C. Duan and M. Yin, *Journal of Alloys and Compounds*, 2014, **588**, 654;

Journal Name

ARTICLE

- 24 M. Peng, N. Zhang, L. Wondraczek, J. Qiu, Z. Yang and Q. Zhang,
Optics Express, 2011, **19**, 20799;
- 25 R. Xie, N. Hirotsaki, M. Mitomo, Y. Yamamoto and T. Suehiro,
Journal of Physical Chemistry B, 2004, **108**, 12027.

